Detection of contrast microbubble shell rupture

A. Ammi[1], R. Cleveland[2], J. Mamou[3], G. Wang[3], L. Bridal[1], W. O'Brien, Jr. [3]

[1] *Laboratoire d'Imagerie Paramétrique, 75006 Paris, France, courriel :bridal@lip.bhdc.jussieu.fr*

[2] *Dept Aerospace and Mechanical Eng., Boston University, 02215, USA*

[3] *Bioacoustics Research Lab., University of Illinois, Urbana, 61801, USA*

Abstract

The goal of this work is to detect experimentally and quantitatively the destruction of Optison™ ultrasound contrast agent (UCA) microbubbles. Two experimental systems were used. The first system consisted of a passive cavitation detector (PCD) with transmitted pulses at one of three frequencies (0.9, 2.8 and 4.6 MHz), one of three pulse durations (3, 5 or 7 cycles) and peak rarefactional pressures from 0.07 to 5.4 MPa. UCAs in solution were diluted so that the transmitted pulse interacted, on average, with a single UCA. The UCA response and acoustic emissions were detected with a 13-MHz center-frequency receiver. The second system consisted of a PCD setup (transmit 7 cycles at 0.99 MHz at peak rarefactional pressures of 0.3 or 0.8 MPa, receive at a center-frequency of 9.8 MHz) coupled to an optical microscope. UCAs were isolated in a 200-µm-diameter cellulose fiber aligned at the focal positions of the transducers and the microscope. Optical data were acquired with a digital camera synchronized to the transmit acoustic pulse. Post-excitation acoustic emissions with broadband spectral content from the PCD time traces were used to characterize UCA destruction thresholds. Microscopic data provided independent confirmation that only a single microbubble was interrogated and whether that was destroyed by the incident acoustic pulse. Results characterize Optison™ destruction thresholds. The PCD technique presented in this work provides a straight-forward evaluation of UCA destruction.

Introduction

Microbubble destruction is an important key to the development of functional and therapeutic UCA applications. By destroying UCAs with a high-amplitude acoustic pulse and then observing the refill of microbubbles at lower acoustic pressure levels, information on the kinetics of flow can be obtained [1, 2]. However, UCA-based blood perfusion quantification by such techniques is hampered by unintentional modification of UCA concentration and size distribution during imaging and the unknown ultrasound backscattered echo contribution to the received signal by microbubble destruction.

Use of UCAs as drug delivery vehicles is also being explored [3]. Local, controlled delivery of drugs such as chemotherapeutic agents should significantly reduce undesirable side effects. Encapsulated microbubbles can be ruptured with an acoustic pulse. Such acoustic destruction of microbubbles designed for transporting therapeutic agents could be applied to UCAs concentrated at a desired treatment site in vivo.

Knowledge of the UCA destruction thresholds is thus important for development of functional imaging as well as UCA-aided drug delivery techniques. Two experimental techniques have predominantly been used to characterize UCA destruction thresholds. The first technique relies on microscopic observations for direct evaluation of UCA destruction. Chomas et al. [4, 5] used a high-speed camera to experimentally observe the destruction or the disappearance of isolated UCAs. Direct, high-speed optical observation provides information not only on destruction thresholds but also concerning the mechanisms for the destruction. However, the expensive equipment necessary for its application limits the technique's accessibility. Furthermore, the delicate alignment needed to isolate a microbubble in the optical and acoustic focal zones limits the throughput of the technique. The second technique is a PCD that uses a receiver to listen passively for acoustic emissions from microbubbles excited by another source. A PCD has been used to determine the UCA cavitation thresholds based on the peak rarefactional pressure amplitude that caused an increase in the broadband noise emission or an increase of voltage "spikes" in the passively received signal [6, 7]. The PCD technique is widely accessible and offers rapid data acquisition. Comparison of threshold levels reported for Optison™ under similar conditions [6, 7], however, reveals that the UCA destruction thresholds that have been reported using PCD detection vary as a function of rather subjective criteria concerning the amplitude of broadband noise and voltage spike increases that indicate bubble destruction.

This work presents experimental investigation of the shell rupture of single UCA microbubbles with two measurement systems (a PCD and a system allowing acoustic interrogation with microscopic observation). A novel criterion [8] based on the detection of post-excitation inertial cavitation (IC) signals is used to detect destruction thresholds. Results enable the quantification of the minimum and the 50% destruction occurrence thresholds for Optison™ at three

incident frequencies (0.9, 2.8 and 4.6 MHz) and three pulse durations (3, 5 and 7 cycles). Observations obtained with the system allowing microbubble isolation with optical verification are presented to validate the signal features associated with rupture in the PCD experiments and are associated with the rupture of single Optison™ microbubbles.

Contrast agent

Experiments were conducted using Optison™ (Mallinckrodt and Molecular Biosystems, San Diego, CA), an FDA-approved UCA. Optison™ microbubbles have an albumin shell, approximately 15-nm thick, encapsulating perflutren C3F8 gas. The solution in the manufacturer's vial has a concentration between 5 and 8 x 10^8 microbubbles/mL. Approximately 93% of the microbubble diameters are less than 10 µm, with a maximum diameter of 32 µm and a mean diameter in the range of 2-4.5 µm [9].

Experimental systems

Passive Cavitation Detector: The PCD setup is described in detail elsewhere [8]. It consists of a passive receiver (13-MHz center frequency) aligned at 70° and confocal to a transmitter (0.9, 2.8 or 4. 6 MHz center frequency). The transducers were immersed in gently stirred water containing a very dilute concentration of UCAs. The transmit transducer was excited with a sinusoidal pulse (3, 5 or 7 cycles) having a peak rarefactional pressure at the transducer focus between 0.07 and 5.4 MPa. The signal received with the passive receiver was amplified, digitized (12-bit, 200 MHz) and saved to a personal computer. For each pulse duration, frequency and pressure setting, the above data acquisition sequence was repeated 128 times. The UCA solution was diluted relative to the confocal detection volume such that, on average, only one UCA microbubble should be interrogated with each incident pulse.

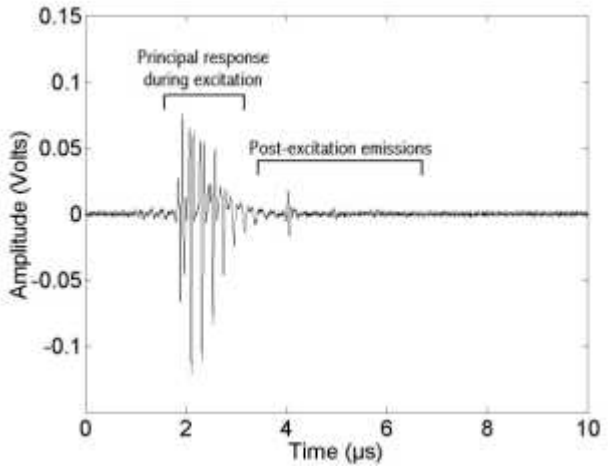

Figure 1: Signal received with the 13-MHz transducer of the PCD system. The principal response corresponds to the acoustic signals received during the insonification of the microbubble by the transmit transducer. Post-excitation signals were detected after the excitation of the microbubble has ceased.

In previous work [8], we demonstrated that post-excitation signals (Figure 1) detected with the PCD were linked to inertial cavitation (IC) and rebound events. Thus, the detection of these signals could be used to evaluate UCA rupture.

Optical/Acoustic measurement system: An optically transparent, 200-µm inner-diameter hollow cellulose fiber (MWCO, Spectrum Labs Inc., Rancho Dominguez, CA, USA) was positioned in a Plexiglas tank containing degassed water. The fiber was positioned with a micromanipulation system (MDT616, ThoroLab, UK). A solution of contrast agent diluted to approximately 1 microbubble/µL was injected with a manual microinjector (IM-5B, Narishige Inc., Japan). This dilution provided for approximately one microbubble per microscopic field of view. A microscope (Z16 APO, Leica, Bannockburn, IL, USA) interfaced to a camera was used for optical observation of the fiber and its contents. A 9.2X zoom level with a 20X objective (Leica Achroplan 100X, NA = 0.42) provided sufficient magnification for the visualization of UCAs microbubbles to approximately 0.8-µm diameter while providing a significant working distance of 20 mm. The large working distance of this objective offers the advantage that no acoustic echoes are reflected by the microscope objective (The objective tip remains above the water's surface). A high-intensity, continuous halogen source (250 Watts, Techni-Quip Inc., Eastlake, OH) was used to illuminate the fiber in transmission. The tank and the microscope were mounted on an active antivibration table (07 OTI 031, Melles Griot Ltd, UK).

The ultrasonic transducers were fit in two orthogonal sides of the tank such that the cellulose fiber was at the focal distance of each and the long axis of the cellulose fiber was at an angle of 45° with respect to the insonification axis of each transducer. A 0.99-MHz measured center frequency transducer (V302, Parametrics, MA) was used to transmit and a 9.8-MHz measured center frequency transducer (ILD-1006-GP, Sofratest, France) was used to receive. The transmit electronics consisted of an arbitrary waveform generator (Agilent 33250A, Thousand Oaks, CA) used to create the pulse train, and an RF power amplifier (ENI A150, Rochester, NY), which amplified (55 dB) the signal sent to the transducer. The signals received with the 9.8 MHz receiver were amplified (BR 640A, Ritec Inc, Warwick, RI) and recorded by a digital oscilloscope (6051A, Lecroy Inc. Chestnut Ridge, NY) controlled by LabView (National Instruments, Austin, TX). Each time trace containing 20000 points at 100 Msamples per second sampled at 8 bits was stored for data analysis using Matlab® (MathWorks, Natick, MA).

A short exposure-time camera was mounted on the microscope (LH 509 ULL, France). The black and white CCD camera captured images with exposure times of 100 ns. Maximum image acquisition frequency was 25 Hz. Images received by the camera were recorded via a digital card (Matrox Meteor-II, Matrox imaging, Canada) and saved to PC using commercial software produced by the camera and card retailers. The spatial resolution was 0.12 µm/pixel and the number of pixels was 768X576 in an image.

Once a moving UCA was optically observed the injection process was stopped and the microbubble was approximately centered in the optical field of view. An excitation at the transducer centre frequency (0.99 MHz) was generated. For each transmit excitation, received signals were acquired with the 9.8-MHz receive transducer and images of the microscope field were digitized with the camera. Figure 2 shows a chronogram of the acquisition sequence.

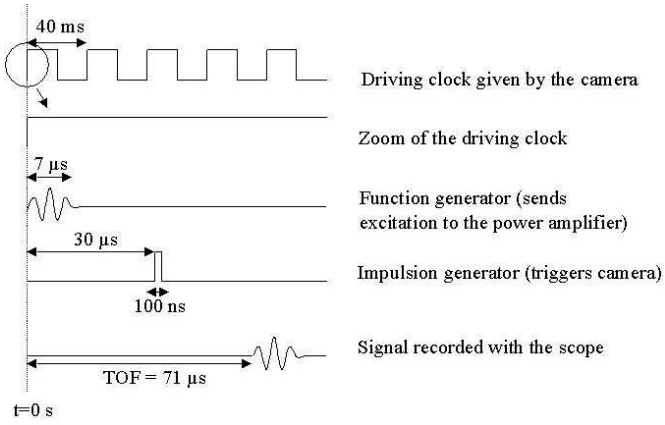

Figure 2: The camera provides the driving clock. The function generator sends an amplified pulse to the transducer when the first rising edge of the driving clock occurs (at t=0). At a selected delay (30 µs in this case), the camera is triggered to record a microscopic image of the microbubble prior to acoustic excitation. The total time-of-flight (TOF) from the transmit transducer to the microbubble to the receive transducer is 71 µs. The signal received by the 9.8-MHz receiver is recorded with the digital oscilloscope from t=0 to 200 µs. The transmit, image and receive sequence is repeated at the next rising edge of the master clock.

Results

PCD evaluation of microbubble rupture

Measured threshold levels are summarized in the Table 1.

Frequency (MHz)	Number of cycles	Minimum rupture threshold (MPa)	50 % destruction threshold (MPa)
0.9	3	0.53	1.26
	5	0.40	1.14
	7	0.29	1.13
2.8	3	0.87	1.74
	5	0.77	1.60
	7	0.71	1.59
4.6	3	0.99	3.19
	5	0.93	2.54
	7	0.89	2.29

Table 1: Thresholds for Optison microbubble destruction.

Based on the lowest peak rarefactional pressure leading to a post-excitation response, the minimum UCA rupture threshold was estimated for each incident frequency and pulse duration. The peak rarefactional pressure leading to destruction of 50% of detected UCAs was identified for each incident frequency and pulse duration. The 50% destruction threshold equals the peak rarefactional pressure for which the number of detected UCAs with post-excitation signals divided by the total number of detected UCAs (oscillating or ruptured) times 100 approaches 50%.

Acoustic/optical evaluation of microbubble destruction

Eleven microbubbles were studied with synchronized optical and acoustic data. Of these, the 5 UCAs exposed to pulses with a peak rarefactional pressure of 0.27 MPa did not present IC signal and remained visible in the microscopic images throughout the experiment. The other 6 UCAs exposed to a peak rarefactional pressure of 0.82 MPa demonstrated post-excitation IC signal (Figure 3). All of the microbubbles without IC signal remained visible in microscopic images throughout the duration of the experiment. All of the microbubbles presenting an IC signal in an acoustic trace were confirmed to be absent in the microscopic image acquired just after the acquisition of the acoustic trace with IC (Figure 4).

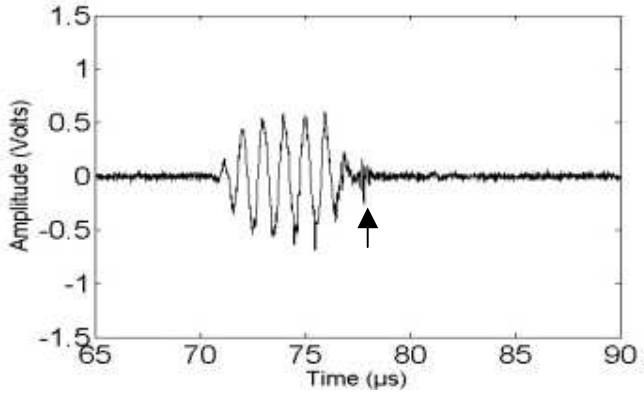

Figure 3: First received waveform with a 9.8-MHz receiver for a 0.99-MHz, 7-cycle, 0.82-MPa peak rarefactional pressure excitation. The post-excitation response is indicated by an arrow.

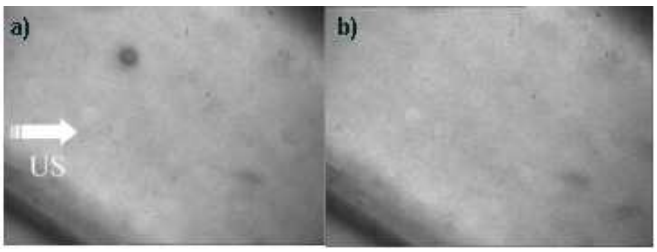

Figure 4: Images of the single microbubble before (a) and after (b) insonification with a 0.82-MPa, 7-cycle 0.99-MHz acoustic pule giving rise to the post-excitation signals presented in Figure 3. The initial radius was estimated to be 4.9 µm at a higher magnification.

The initial diameter of the 6 destroyed microbubbles (evaluated on the microscopic images prior to insonification) ranged from 2.6 to 8.5 µm. Microbubbles with larger initial diameters presented a higher peak-to-peak voltage amplitude during the principal response. The time delay between the IC signal and the end of the principal response did not vary detectably as a function of the initial microbubble size.

Discussion

The current work extends previous estimates of the minimum peak rarefactional pressure leading to a single microbubble rupture event to estimate the 50% occurrence of microbubble rupture as a function of pressure. Except for the case of 7 cycles at 0.9 MHz, the 50% threshold was on the order of 2 to 3 times higher than the minimum rupture threshold measured at the same frequency and pulse duration. Knowledge of pressure thresholds for a range of microbubble destruction levels should contribute to selecting the pulse characteristics best adapted for imaging (minimized microbubble destruction) and therapeutic (maximized or controlled destruction) applications.

Additional information was gained by coupling a PCD to an optical microscope. For the measurements reported with the PCD system, the microbubbles were freely circulating in a tank. In the optical/acoustic setup, stationary microbubbles were isolated in a cellulose tube. This setup allowed to verify optically that only a signal microbubble was present at the measurement site and that the microbubble disappearance was well correlated with the detection of post-excitation signals. The images obtained with the microscope were also used to provide an estimate of the equilibrium microbubble size prior to insonification. This information should allow more precise comparison between experimental results and theoretical models for microbubble wall movement. Future work should apply this experimental system to determine pressure thresholds for destruction as a function of the initial microbubble radius. The combination of optical and acoustic techniques provides a powerful tool for UCA characterization. This combination is made possible, without interference in the ultrasonic field, because of the large working distance offered by the selected microscope objective.

To date, theoretical analysis of the destruction process has been based on approximate instability criteria developed for free bubbles. A rigorous analysis of the mechanical behavior of the shelled UCAs during destruction has not been reported. More extensive experimental data should help develop theoretical models for UCA microbubble destruction. The data describing pressure thresholds for shell rupture described in this work can be used to test and adjust such models.

The PCD system enables rapid throughput for the assessment of microbubble rupture thresholds, and its use should help to assess rupture thresholds for a large variety of incident acoustic parameters and for different ultrasound contrast agents.

References

[1] Quantification of myocardial blood flow with ultrasound-induced destruction of microbubbles administered as a constant venous infusion. Circulation 97 (1998), 473-483

[2] Effect of microbubble exposure to ultrasound on quantitation of myocardial perfusion. Echocardiography 22 (2005), 503-509

[3] Assessment of endogenous and therapeutic arteriogenesis by contrast ultrasound molecular imaging of integrin expression. Circulation 111 (2005), 3248-3254

[4] Threshold of fragmentation for ultrasonic contrast agents. J Biomed Opt 6 (2001), 141-150

[5] Mechanisms of contrast agent destruction. IEEE Trans Ultrason Ferroelectr Freq Control 48 (2001), 232-248

[6] Ultrasound-mediated cavitation thresholds of liquid perfluorocarbon droplets in vitro. Ultrasound Med Biol 29 (2003), 1359-1365

[7] A comparison of the fragmentation thresholds and inertial cavitation doses of different ultrasound contrast agents. J Acoust Soc Am 113 (2003), 643-651

[8] Ultrasonic contrast agent shell rupture detected by inertial caviation and rebound signals. IEEE Trans Ultrason Ferroelectr Freq Control 53 (2006), 126-136

[9] Physical and biochemical stability of Optison, an injectable ultrasound contrast agent. Biotechnol Appl Biochem 30 (1999), 213-223